

Replacing the solid needle by a liquid one when measuring static and advancing contact angles

Ming Jin¹ · Raymond Sanedrin² · Daniel Frese¹ · Carsten Scheithauer¹ · Thomas Willers¹

Received: 7 October 2015 / Revised: 2 December 2015 / Accepted: 18 December 2015 / Published online: 11 January 2016
© Springer-Verlag Berlin Heidelberg 2016

Abstract In general, the optical determination of static and advancing contact angle is made on drops applied or extended, respectively, onto a substrate through the use of thin solid needles. Although this method is used extensively, this way of dosing can be time consuming, cumbersome and if not performed meticulously can lead to erroneous results. Herein, we present an alternative way of applying drops onto substrates using a liquid jet produced by a liquid pressure dosing system acting as a “liquid needle”. We performed a comparative static contact angle study on 14 different surfaces with two different liquids (water and diiodomethane) utilizing two different ways of dosing: the conventional solid and a novel liquid needle-based technique. We found, for all but one sample, that the obtained results on μl size drops were comparable within the experimental error bars provided the liquid needle is thin enough. Observed differences are explained by the special characteristics of either way of dosing. In addition, we demonstrate how the liquid pressure-based dosing system facilitates high-speed optical advancing contact angle measurement by expanding a drop from 0.1 to 22 μl within less than 1.2 s but yet providing constant contact angle versus drop base diameter curves. The obtained results were compared with data from tensiometric dynamic Wilhelmy contact angle measurements. These data, in conjunction with sequences of

live images of the dosing process of the liquid pressure dosing system, illustrate how this system can replace the solid needle by a liquid needle.

Keywords Contact angle · Advancing contact angle · Liquid needle · Self assembled monolayers

Introduction

Contact angle phenomena are one fundamental topic in physics and its measurement is of great relevance in the large multidisciplinary field of surface and interface science for a vast range of industrial and practical applications and scientifically motivated questions. Optical contact angle (CA) measurements are as old as Young’s equation [1], which is more than two centuries. Since then, advances in this experimental technique have been made: The last revolutionary input had been the introduction of digital image processing in the 1990s [2] and automated liquid-dosing and needle-moving systems have become common. Thanks to these, the optical determination of contact-angle hysteresis [3] and, in particular, a precise optical determination of the advancing contact angle have become possible. However, the method by which the liquid is applied on a solid surface for the static contact angle determination has not changed. Typically, a dosing mechanism generates a pendant drop at the tip of a needle and is subsequently carefully moved downward to the solid substrate until the liquid drop touches the surface. Gravity, in addition to work of adhesion, causes the droplet to detach from the tip of the needle, and it is transferred on the substrate surface. This method can become cumbersome or even erroneous for instances wherein the needle is moved too far towards the substrate. This results to squeezing and forcing the sessile drop on the

✉ Thomas Willers
T.Willers@kruss.de

¹ KRÜSS GmbH, Borsteler Chaussee 85, 22453 Hamburg, Germany

² KRÜSS USA, 1020 Crews Road, Matthews, NC 28105, USA

surface and consequently an underestimation of the contact angle. This is particularly important for hydrophobic samples exhibiting a considerable contact angle hysteresis [4]. For example, the water contact angle on the same surface of polydimethylsiloxane (PDMS) can vary between 108° and 114° depending on how close the needle was moved towards the substrate. Kwon et al. showed that even for careful use of the well-established solid needle deposition technique, transitions of wetting states can occur that go along with drastic changes in observed contact angles [4]. Furthermore, the effect of the solid needle inside the droplet, which has been shown to have an influence on both the dynamic and static contact angle, is also frequently discussed and is particularly important for superhydrophobic surfaces [5–7]. Moreover, this method of drop deposition often takes more than a few seconds if the abovementioned possible errors should be avoided. An already existing needle-less and quicker alternative is to shoot individual separate drops onto the surface [8] or simply letting μl -size drops fall down onto the substrate. However, the liquid drops impact onto the substrate with non-negligible high kinetic energies (Weber numbers) [9–14]. This influences particularly the contact angle results on surfaces with larger contact angle hysteresis, which often makes them not comparable to contact angle data recorded with a needle-based dosing system (NDS).

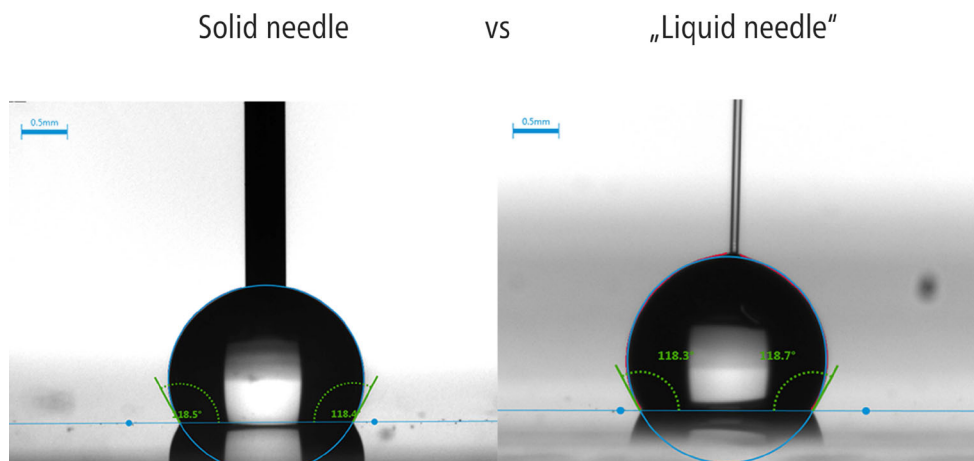
Herein, we present a way of applying drops onto the surface using a continuous liquid jet build up by a liquid pressure-based dosing system (PDS). To the best of our knowledge, this method has not been established in the field of optical contact angle analysis thus far. This is because usually the liquid jet needs to have a high speed (i.e., high Weber number) in order to form a continuous jet. The high kinetic energy is suspected to have a considerable influence on the contact angle results. More precisely, if the liquid jet is hitting the substrate with too high speed (i.e., kinetic

energy), it first splashes over the substrate and then contracts to form a droplet. As a result, the measured contact angles appear to be less reproducible and more importantly are the result of a de-wetting process which is in contrast to the contact angles measured with a traditional needle-based system, where the result of a spontaneous wetting process is observed. In addition, a break-up of the liquid jet before hitting the substrate can cause the formation of air bubbles inside the drops also falsifying the contact angle results.

The PDS used for this study is designed such that it works just at the right balance to have a sufficiently high flux of the liquid in order to form a jet hitting the substrate but still low enough so that influences of the kinetic energies on the measured contact angles become negligible [15]. Hereby, it overcomes the above mentioned obstacles. The liquid jet builds up the droplet on the substrate similar to a solid needle whose tip is slightly above the substrate surface. In this way, the solid needle is replaced by a *liquid needle*, as it is exemplarily illustrated in Fig. 1.

Herein, we will present and discuss a comparative study of static contact angles on a large range of different solids obtained with the traditional solid needle-based dosing mechanism and the liquid pressure based-dosing mechanism, i.e., the liquid needle. For many applications, static contact angle measurements provide already enough information. However, there are also many applications and scientifically motivated questions for that information of the advancing contact angle were shown to be more relevant and examples for this can be found in the cited literature [16–18]. Therefore, we will additionally present how the liquid needle facilitates high speed, highly reproducible advancing contact angle measurements. These optical dynamic contact angle measurements will also be compared with force-based measurements using the Wilhelmy method.

Fig. 1 (color online) Exemplary images of a droplet dosed by a conventional solid needle dosing system NDS (left image) and by the novel liquid needle (right image) technique using the KRÜSS liquid pressure dosing system PDS. The blue scale in the upper left corner of each image represents 0.5 mm. The red line is the drop contour as detected by the KRÜSS ADVANCE software. The blue line is a Tangent-1 fit to the drop contour. The green lines represent the contact angles determined from that fit



Experimental

Samples investigated

We have investigated 14 different solid surfaces. We chose very different material qualities, from almost ideally chemically homogeneous surfaces and technical raw materials to finished commercial products. All samples were flat. Table 1 summarizes all samples investigated. The PDMS samples were prepared from Sylgard 184 (Dow Corning, Wiesbaden, Germany) Briefly, the resin component and the curing agent were mixed in a 10:1 ratio and poured into a clean glass vessel. After 30 min, the mixture was cured for 1 h at 100 °C. For experiments performed according to the Wilhelmy plate method, cured PDMS samples were punched into rectangular pieces. Planar polyethylene (PE) samples were prepared by melting of PE pellets (LDPE, melt index 25 g/10 min at 190 °C, Sigma Aldrich, Steinheim, Germany) in an aluminum cup at 170 °C for 3 h and successive overnight cooling. The surface of the resulting PE block was treated with sandpaper (Starcke Matador 991A P1500, Starcke GmbH & Co. KG, Melle, Germany) to reduce its roughness. Commercially available sandpaper (Starcke Matador 991A P500, P1000 and P1500, Starcke GmbH & Co. KG, Melle, Germany) with different grain sizes was silanized with Fluka silanization solution (5 % dimethyldichlorosilane in heptane, Sigma Aldrich, Steinheim, Germany). The sandpaper was immersed in the silanization solution for 6 h, followed by 2 h of drying under ambient conditions. The P2I-plasma-treated filter paper was kindly provided by P2i Limited, Abingdon, UK.

Organosilane self-assembled monolayers (SAMs) formed on surfaces have been extensively used in the past, and the free functional group moieties of the formed

monolayer are used to modify the physical and chemical properties of surfaces. Organosilane SAMs were deposited following published protocols [19, 20]. Briefly, silicon oxide (SiO₂) strips with dimensions of 1.5 × 0.5 cm (L × W) were cut from ultra-flat (SiO₂) wafer and were subsequently sonicated in water, isopropanol, and ethanol for at least 30 min in each solvent. The (SiO₂) strips were then dried with low stream of air. To form the organosilane SAMs, the substrate strips were immersed in a 2.5 % solution in toluene of dichlorodimethylsilane (DDMS) or 5 % solution in ethanol/water (95:5) of aminopropyltrimethoxysilane (APTMS) for a minimum of 12 or 3 h, respectively. The functionalized (SiO₂) strips were then thoroughly rinsed with either toluene or ethanol and isopropanol. Substrates were then baked at 100 °C for 15 min and cooled down for 10 min. Contact angles were then measured within 30 min.

For all samples except for the functionalized and silanized samples, the same cleaning procedure was applied prior to the measurement: first cleaned with a degreasing detergent solution and then rinsed thoroughly with hot and cold tap water and finally with distilled water. Remaining water drops were subsequently removed with isopropanol. The samples were finally dried with clean compressed air. The functionalized and silanized samples were rinsed with isopropanol and dried in a clean air stream before the contact angle measurement.

Experimental methods

All contact angle measurements were carried out using a KRÜSS Drop Shape Analyzer-DSA100. For the experiments with the solid needle-based dosing system, a software controlled fully automatic drop deposition technique was used in order to guarantee that every drop had the same

Table 1 Solid samples investigated

Description	Quality	Designation
Si wafer	Finished product	Wafer-1
Si wafer	Finished product	Wafer-2
Polydimethylsiloxane	Pure, synthesized	PDMS
P2I-treated filter paper	Finished product	P2I paper
Polypropylene	Finished product	PP
Glass microscope slide	Finished product	Glass
Polyamide 6, atmospheric plasma treated	Finished product	PA6
Polyethylene	Pure, synthesized	PE
Silanized sand paper (500 grain size)	Finished product	Sand paper (500)
Silanized sand paper (1000 grain size)	Finished product	Sand paper (1000)
Silanized sand paper (1500 grain size)	Finished product	Sand paper (1500)
Smartphone display	Finished product	Display
Dichlorodimethylsilane SAMs on SiO ₂ Surface	Pure, functionalized	DDMS SAMs
Aminopropyltrimethoxysilane SAMs on SiO ₂ Surface	Pure, functionalized	APTMS SAMs

volume and was deposited in the same way (i.e., same moving speed of needle, same minimum distance between needle and substrate). In this way, effects on the contact angle of the way how the drop is deposited are minimized resulting in minimum standard deviation. For the experiments with the liquid needle-based dosing, we used the KRÜSS pressure-based dosing system (PDS) DO3252 [15]. For every sample, we measured the static contact angles of two liquids, bidistilled water and diiodomethane (Sigma Aldrich, ReagentPlus, 99 %). There were no time-dependent changes in the contact angle for any of the samples except for diiodomethane (DIM) on PDMS. Here, the static contact angle measured with both dosing system was recorded at the same time after drop deposition was finished.

Water contact angles were measured for drop volumes of 1 and 3 μl in order to cover a range of volumes guaranteeing that the obtained drop base diameters (DBD) are well below the corresponding capillary length scale $\sqrt{\sigma_l/(\rho g)} \approx 2.7$ mm, with σ_l , ρ , and g being the surface tension, density of the liquid, and the gravitational constant, respectively [21]. DIM contact angles were measured for drop volumes of 1 μl . Owing to the larger density of DIM (three times that of water), the capillary length scale of DIM is reduced by a factor 0.57 compared to water. Only for glass, we measured additionally DIM drops with a volume of 2.5 μl . For every sample and dosing system, a minimum of 20 separate drops per liquid and drop volume were measured. All experiments were performed under ambient conditions. For each different sample, the same light settings and fitting algorithm were used. The used algorithms were Tangent-1 (T-1), circle, and height-width as implemented in the KRÜSS ADVANCE software. For further statistical evaluations, the mean contact angle as calculated from

the left and right hand side contact angle of every different drop was used. The fully automatic measurement of 20 drops using the solid and liquid needle-based system usually took around 220 and 54 s, respectively. It is interesting to note that unlike the NDS the PDS DO3252 can dose and analyze two separate drops simultaneously. The optical advancing contact angle measurements were done automatically by the KRÜSS ADVANCE software, which analyzed every image recorded by the camera during the dosing process. Depending on the dosing mechanism frame rates up to 122 fps had been used. For the dynamic Wilhelmy contact angle measurements, we used a KRÜSS Force Tensiometer-K100. The immersion speed (i.e., speed of contact line) was set to 0.2 and 1 mm/min for the PDMS and APTMS SAMs samples, respectively.

Results and discussion

Static contact angles

A comparison of the static water contact angles measured on all samples using different drop volumes and dosing mechanism is shown in Fig. 2. The open columns represent the contact angles of drops deposited with the NDS and the filled columns show the ones with the PDS, i.e., the liquid needle. The error bars reflect the standard deviation of the mean value calculated from a minimum of 20 separate drops. All obtained standard deviations are in the range of 0.4° (1 μl drop dosed with NDS on DDMS SAMs) to 3.6° (3 μl drops dosed with PDS on glass). For both dosing systems, the way how the liquid is applied onto the substrate were well controlled thus reducing the experimental error caused by different ways of drop deposition to a minimum.

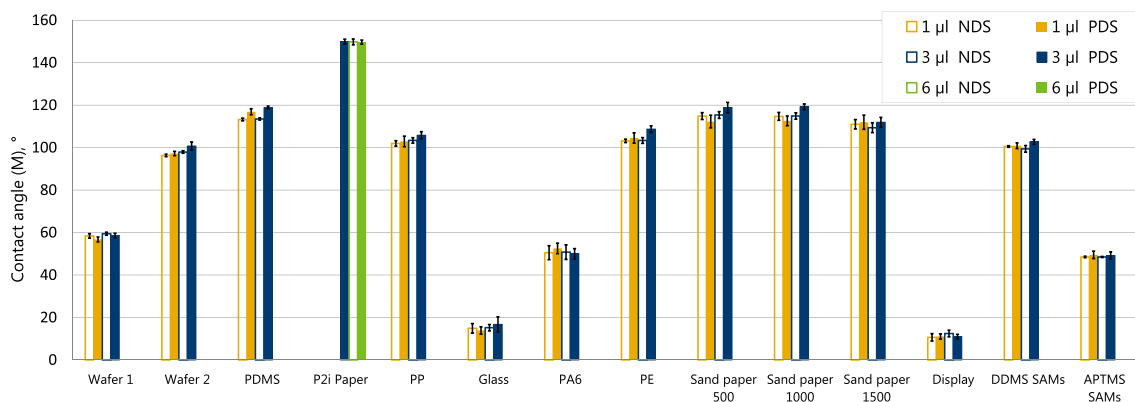


Fig. 2 (color online) Mean static water contact angles as measured after dosing with the solid needle dosing system NDS (open columns) and the liquid needle, i.e. the pressure dosing system PDS (filled columns) for 1 μl (yellow, bright) and 3 μl (blue, dark) drops on all

samples investigated. For the P2i Paper sample drops with a volume of 6 μl (green) are also shown. The error bars reflect the standard deviation as obtained from a minimum of 20 different drops measured

As a result, the error bars mostly reflect the inhomogeneity of the sample surfaces. This is supported by the fact that the functionalized wafer, a chemically homogeneous and topographically very smooth surface exhibits error bars at the lower end of this range with a maximum value of 1.6° for the $3\ \mu\text{l}$ drops deposited with the PDS. Similarly, for most measured samples and volumes, the observation that the magnitude of the error bars are comparable independent of the used dosing mechanism indicates that the magnitude of the error bars do not depend significantly on the method of dosing.

With all examined samples, we covered a range of contact angles between 10° (display) to 150° (P2I plasma treated filter paper). The contact angles measured on DDMS and APTMS SAMs agree well with those reported on equally prepared samples [19, 20]. With the exception of PDMS, the contact angles measured on $1\ \mu\text{l}$ drops dosed with both systems are in agreement within the experimental error bars. For $3\ \mu\text{l}$ drops, only the contact angles on PDMS, PE, and the sand paper (grain size of 1000), were not in agreement within the error bars when comparing both dosing mechanisms. The observed difference for the sand paper sample is very small, which suggests that this is not caused by using either dosing systems but rather by normal experimental error due to sample inhomogeneity. In contrast, the PDMS sample, which is physically very smooth, exhibited a significant difference of about 5° between the two dosing systems. Interestingly, for both investigated drop volumes, the contact angle measured on drops deposited by the liquid needle (i.e., PDS) is larger than by the NDS. Presumably, this is related to the considerably large hysteresis of the water contact angle on PDMS of about 60° (compare Fig. 6), i.e., there are pronounced pinning effects for the water contact line on this substrate. The fact that the contact angles for the liquid needle-based dosing system are larger indicates that this method applies a droplet with even less kinetic energy than the NDS. When the drop is applied with the solid needle, the gravitation (i.e., additional kinetic energy) helps the drop to wet more surface of the PDMS than would be wetted by a purely work of adhesion driven wetting. Due to the large contact angle hysteresis (i.e., pinning forces), the contact line does not retract after all the initial kinetic energy has dissipated. For the PDS, this does not happen, i.e., the contact line does not move so far from the center of the drop and therefore the measured contact angle is larger. Thus, for the PDS, the effects of additional kinetic energies on the contact angle are even reduced compared to the solid needle-based system. We consider this as a strong point of the PDS as it can provide information on a more purely work of adhesion driven wetting not influenced by an additional forceful expansion of the drop. However, for most samples having a smaller contact angle hysteresis, this difference was observed to be negligible.

Interestingly, the contact angles measured on the three equally silanized sand papers with grain sizes (i.e., roughnesses) of 500, 1000, and 1500 do not exhibit significant differences between the different dosing mechanism. This suggests that irrespective of dosing method macroscopically rough surfaces yield comparable results.

The contact angle results of the P2I plasma treated filter paper demonstrate a neat advantage of the PDS over the NDS. Figure 2 shows only results of $6\ \mu\text{l}$ volume drops deposited with the NDS on this super hydrophobic, i.e., low surface free energy sample (water contact angle of about 150°). For this sample, only water droplets with a minimum volume of $6\ \mu\text{l}$ could be deposited with the NDS. For smaller volumes, the drop did not detach from the needle. With increasing drop volume the contour length scale of the liquid being in contact with the solid substrate increases as it still hangs at the tip of the needle. As a result, the drop-surface adhesive force is greater than the drop-needle adhesive force [5] which makes the drop detach from the needle, i.e., the substrate wins the battle in work of adhesion over the needle. However, for the PDS, this is not applicable and as shown in Fig. 2, $3\ \mu\text{l}$ drops could be deposited using the PDS. This way the liquid needle-based dosing system facilitates volume dependence studies on hydrophobic substrates over a larger volume range down to smaller volumes not accessible with a traditional NDS.

Figure 3 shows a corresponding comparison of the measured contact angles of $1\ \mu\text{l}$ DIM drops on the same samples. Even though the error bars for the DIM contact angles were for most samples smaller than for the water measurement, the measured contact angles obtained by both dosing systems are in agreement for all samples except for wafer-1 and glass samples. For wafer-1, the difference is only minimal in relation to the magnitude of the errorbars. However, the DIM contact angle on glass measured with the PDS is about six degrees smaller than the one measured with the standard NDS. Considering that the density of DIM is tripled compared to that of water, this difference suggests that, for the glass sample, the effect of the kinetic energy on the contact angle is larger using the PDS than the NDS resulting to the liquid wetting a larger surface area and thus a smaller contact angle. However, how the effect of the kinetic energy of the liquid dosed with a liquid jet on the substrate affects the contact angle depends on the flux of the liquid jet and the ratio of the diameter of the jet compared to the drop base diameter (DBD) [15]. The smaller the ratio of diameter of the liquid jet compared to the DBD, the less influence the kinetic energy has on the resulting contact angle. Simply spoken, the kinetic energy of the liquid jet dissipates over larger volumes (i.e., liquid's mass) and thus less affects the three phase contact line, i.e., the contact

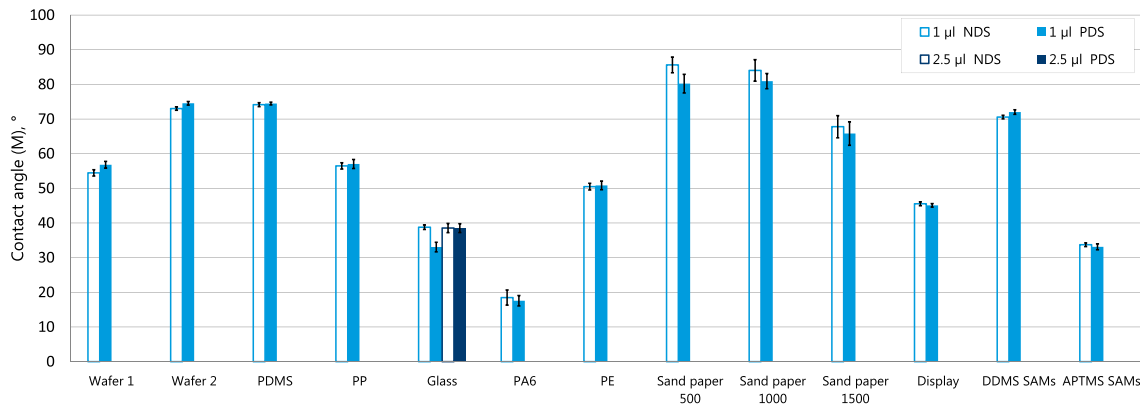


Fig. 3 (color online) Mean static diiodomethane contact angles as measured after dosing with the solid needle dosing system NDS (open columns) and the liquid needle, i.e., the pressure dosing system PDS (filled columns) for 1 μl drops on all samples investigated. For the

glass sample 2.5 μl drops were also measured. The error bars reflect the standard deviation as obtained from a minimum of 20 different drops measured

angle. In order to experimentally support this idea, Fig. 3 shows additional results for DIM contact angles on the glass sample for drop volumes of 2.5 μl . As the volume of the drops increases, the difference in contact angle observed by the two different dosing mechanisms becomes smaller than

the experimental error bars. This effect of a too large ratio of liquid needle diameter to DBD on the contact angle can also be nicely seen by a detailed look on the dynamic contact angle measurement done with the PDS discussed and shown below.

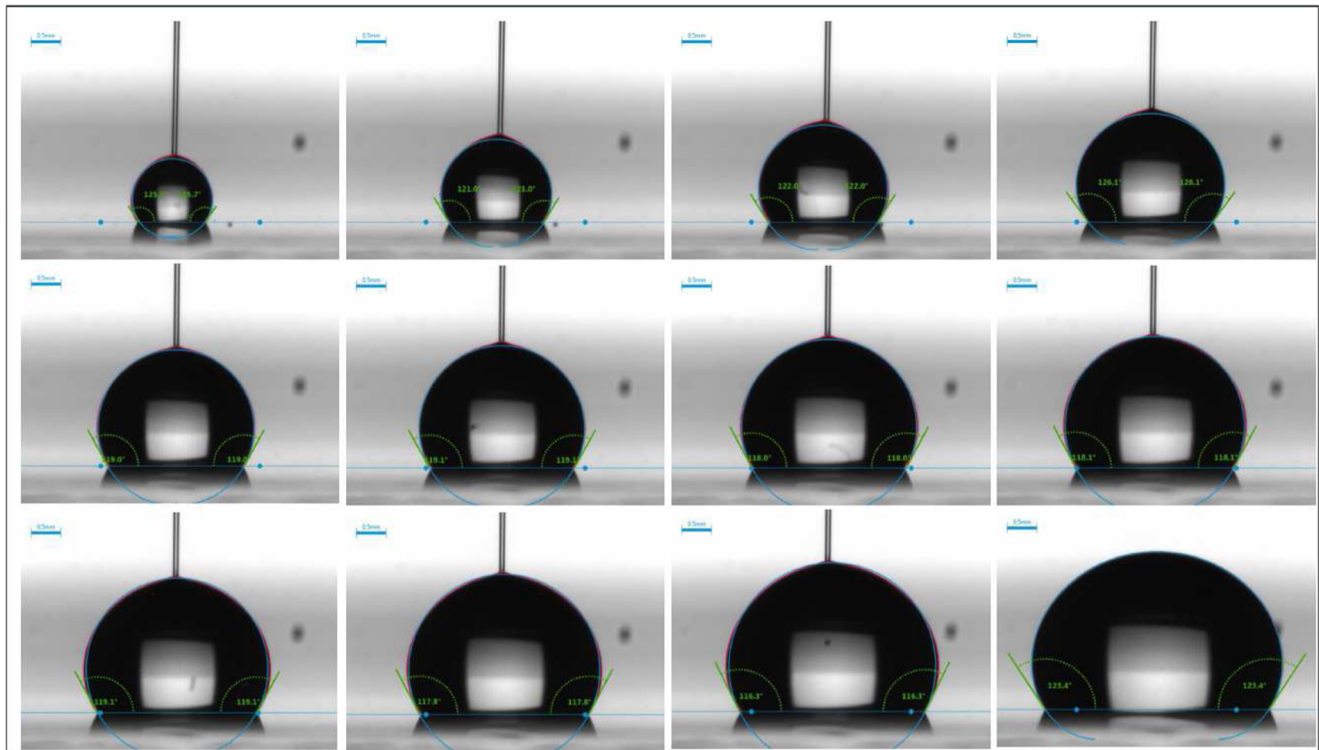


Fig. 4 (color online) Sequence of images illustrating the dosing process when a 22 μl water drop is dosed on PDMS using the liquid needle, i.e., PDS. The total time of the dosing process was 1.15 s. The blue scale in the upper left corner of each image represents 0.5 mm.

The red line is the drop contour as detected by the KRÜSS ADVANCE Software. The blue line is a Young-Laplace fit to that drop contour. The green lines represent the contact angles determined from that fit

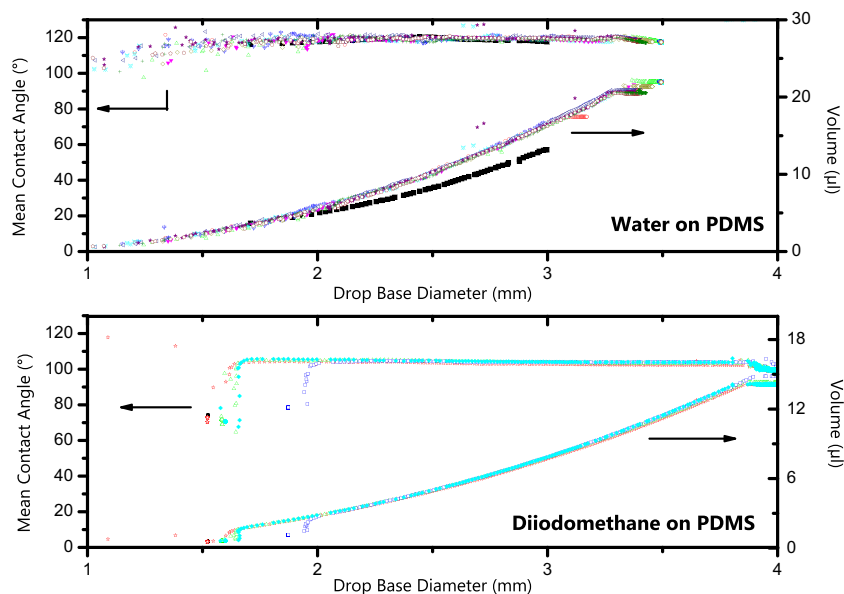


Fig. 5 (color online) Dynamic contact angle measurements of water (*top panel*) and diiodomethane (*bottom panel*) on PDMS performed with the liquid needle dosing system, i.e., PDS. The mean contact angle as calculated from the left and right hand side contact angles and the drop volume are plotted as a function of the drop base diameter. In the top panel, curves obtained from 10 different measurements are

shown by the *colored symbols*. In addition, the results from one measurement done with the NDS are shown as full *black squares*. In the bottom panel, the results of four different measurements are shown. Each measurement performed with the liquid needle took less than 1.15 s

Dynamic contact angles

Figure 4 shows some representative raw data images together with the fitted drop contour curves for one single advancing contact angle measurement. From these, it can be nicely seen how the liquid jet acts like a very thin liquid needle that increases the drop volume over time with a continuously forward moving contact line. The upper panel of Fig. 5 shows the mean value of the advancing contact angles on the left and right side of the droplet and the drop volume as a function of the DBD for ten different measurements of water on PDMS. These curves CA versus DBD show that at the beginning of the dosing process until a DBD of about 2 mm has been reached, the values of the contact angles increase from around 105° to 120° . In addition, the scattering of the data obtained from the ten different measurements is rather large at the beginning of the dosing process. The latter can also be seen in the first four images in Fig. 4. However, starting from a DBD of about 2 mm, the advancing contact angle stays constant at 120° and is highly reproducible as seen from the curves of the ten separate measurements lying almost on top of each other. The mean contact angle was calculated from all contact angles measured during an advancing contact angle experiment starting from a DBD of 2 mm. The obtained values from all 10 measurements range from 119.0° to 120.0° for the mean and from

0.7° to 1.5° for the standard deviations. The standard deviations are in the same range as the ones obtained from the static contact angle measurements supporting the idea that the rather high flux of the liquid needle does not cause any additional effects on the result of the dynamic contact angles as long as the ratio liquid needle diameter (LND) to DBD is small. This is also supported by the fact that the detected drop contours in Fig. 4 are reasonably well described by the Young-Laplace function. The slight underestimation of the Young-Laplace fit in Fig. 4 allows approximating how little the drop shape is affected by the fluid dynamics during dosing. After dosing is finished, the drop shape is perfectly described by the Young-Laplace function as shown in the last image of Fig. 4. Using a different less restricted fitting function (e.g., Tangent-2), the drop shape is perfectly fitted at all times during dosing (images not shown here). The initially obtained lower contact angles at the beginning of the dosing process indicate how the in relation to the drop size relatively high kinetic energy affects the contact angle. However, as already observed and discussed in the previous section, these effects become negligible if the ratio of the LND to the DBD decreases. A single measurement on a droplet expanded to a volume of $22 \mu\text{l}$ was completed after 1.15 s and from which the speed of the moving contact lines was calculated to be approximately 1.1 mm/s.

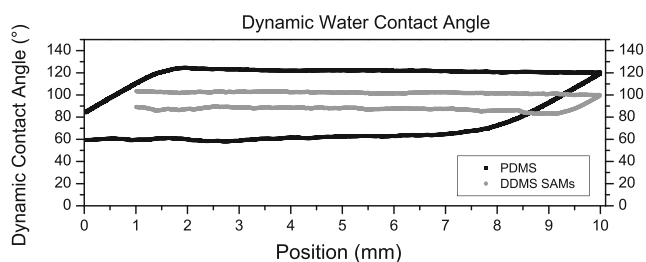


Fig. 6 Dynamic water contact angle measurements on PDMS and DDMS SAMs as measured with the KRÜSS Force Tensiometer-K100 using the dynamic Wilhelmy method. The immersion speed (i.e., speed of contact line) was set to 0.2 and 1 mm/min for the PDMS and APTMS SAMs samples, respectively

For water on PDMS, we also measured the dynamic contact angles using the two already established techniques: expanding droplet using a solid needle and Wilhelmy Force measurements. The data of the expanding droplet measurement is also included in Fig. 5 as filled black squares. The results of the contact angle are in good agreement with the contact angle measured with the PDS. The volume vs. DBD curve shows a smaller slope which can be explained by the solid needle flattening the drop shape and thus resulting in smaller volume to DBD ratios. This type of advancing contact angle measurement took about 25 s which corresponds to a speed of the moving contact lines of about 0.03 mm/s. The measured advancing and receding contact angle versus position using the Wilhelmy Force method is shown in Fig. 6. Here, the speed of the contact line was precisely 0.2 mm/min, thus 3.3×10^{-3} mm/s. The advancing contact angle depends on the speed of the contact line [3, 21, 22]. Interestingly, for water on PDMS, all three different methods each with a speed of the contact line in a different order of magnitude exhibit a comparable advancing contact angle of 120°.

The bottom panel of Fig. 5 shows four different advancing contact angle measurements for diiodomethane on PDMS. The speed of the contact line was comparable to that of the water measurements. Similar to the results obtained for water, all four curves exhibit an increase in the measured contact angle until a DBD of about 2 mm has been reached. Subsequently, a further increase in the DBD resulted in a constant advancing contact angle of 103°. The obtained mean contact angle values calculated from values for a DBD >2 mm range from 102.2° to 104.4° each with a

corresponding standard deviation smaller than 0.65°. We consider this as a very good reproducibility for this type of high-speed advancing contact angle measurements.

In addition to the advancing contact angle measurements using NDS and PDS on PDMS, we performed similar measurements on DDMS SAMs formed on an ultra-flat (SiO₂) surface. We performed five dynamic water and DIM contact angle measurements using the liquid needle. The measurement curves show a qualitatively similar behavior to those obtained on PDMS (curves not shown). Analogous to the analysis for PDMS, we calculated the mean and standard deviation of each single experiment where only contact angle values from liquid drops with a DBD larger than 2 mm were considered. The obtained mean values for DDMS SAMs range from 102.0° to 103.5° with corresponding standard deviations smaller than 2.2° and from 78.6° to 79.8° with corresponding standard deviations smaller than 1.3° for water and DIM, respectively. In addition, we performed 11 dynamic water contact angle measurements using the NDS. Similarly, we calculated the mean over all different position measured in each single advancing contact angle measurement not taking into account the initial increase of contact angle. The obtained mean values range from 100.1° to 104.4° with corresponding standard deviations smaller than 1.2°. Figure 6 shows the advancing and receding contact angle of water on DDMS SAMs using the single side Wilhelmy Force method of the Force Tensiometer-K100. A global mean value for each different sample and type of measurement was calculated from the obtained mean values and summarized in Table 2. As for PDMS, for DDMS SAMs, we also found that the water advancing contact angle measured with the liquid needle and thereby on a fast forward moving contact line is comparable to the one measured with the solid needle and with the Wilhelmy force method, i.e., for a considerably slower forward moving contact line.

Finally, we want to note that the receding contact angle cannot be measured by this liquid needle dosing system. However, we believe that receding contact angles measured using a solid needle are often ill-defined as the distance between solid needle and the substrate can have a significant influence on the result and that receding contact angle measurement are much better defined when the Wilhelmy method is used. In case optical receding contact angle measurements are needed, tilting table experiments can provide a better defined option.

Table 2 Global mean values obtained from advancing contact angles measurements using the pressure dosing (PDS), the needle dosing system (NDS), and the Wilhelmy Force method for PDMS and DDMS SAMs

Sample	Water - PDS	DIM - PDS	Water - NDS	Water - Wilhemly
PDMS	(119.5±1.1)°	(103.7±0.8)°	120°	120°
DDMS SAMs	(102.9±2.0)°	(79.2±0.8)°	(103.5±2.4)°	103°

Conclusions

We present a thorough comparative study of static contact angles measured on a variety of different samples for the liquid drops deposited using two fundamentally different techniques: the traditional solid needle and a liquid pressure-based dosing systems. We illustrate how the latter carefully doses the droplet on the substrate surface with a thin liquid jet acting as liquid needle. We found that the measured static contact angles using either technique are in agreement for almost all samples. This and the few significant differences in contact angle measured by the two techniques were explained by the special characteristics of the pressure-based dosing system. The liquid jet is designed such [15] that its flux is as low as possible but still high enough in order to have a continuous liquid jet hitting the substrate and with a thin diameter resulting in a very low ratio of LND to DBD. Our experimental data support the idea that the corresponding kinetic energy of the liquid jet is dissipated over a sufficiently large drop volume guaranteeing that this kinetic energy has a negligible influence on the contact line and thus the contact angle of the droplet. In conclusion, using this specially equilibrated liquid needle for optical static contact angle measurements is as independent of additional kinetic energies affecting the contact angle as a carefully performed experiment with a solid needle. Sessile drops (1 to 3 μl volume) deposited by the the liquid needle are comparable to those deposited by the way in which a pendant drop on a solid needle is carefully brought into contact with the substrate.

In addition, we demonstrated how this liquid needle facilitates high-speed advancing contact angle measurements which are highly reproducible. And although the measurements are very fast resulting in a very fast forward moving contact line, the drop can be continuously and reasonably well described by the Young-Laplace function during the whole dosing process.

This experimental work provides a sound set of data and can be the motivation for future more theoretical works about this method of dosing using a liquid needle for static and advancing contact angle measurements. In addition, the liquid needle dosing process is much faster (less than 100 ms for dosing a 2 μl drop) as when using a solid needle and is better experimentally defined. Thus, possible errors due do different ways of how the drop is deposited on the substrate as they can occur for the NDS are intrinsically excluded. Furthermore, it enables low kinetic energy deposition of drops on super hydrophobic surfaces. Therefore, we believe that replacing the solid needle by a liquid will become more advantageous for many contact angle studies

and may become another standard method for optical contact angle measurements.

Acknowledgments The authors are thankful to Igor Kogut and Prashant R. Waghmare for fruitful discussions.

Compliance with Ethical Standards

Disclosure of potential conflicts of interest The authors are employed by KRÜSS GmbH.

References

1. Young T (1805) *Phil Trans R Soc Lond*:65–87
2. Cheng P, Li D, Boruvka L, Rotenberg Y, Neumann A (1990) *Colloids Surf* 43(2):151. doi:10.1016/0166-6622(90)80286-D
3. Eral H, 't Mannetje D, Oh J (2013) *Colloid Polym Sci* 291(2):247. doi:10.1007/s00396-012-2796-6
4. Kwon HM, Paxson AT, Varanasi KK, Patankar NA (2011) *Phys Rev Lett* 106:036102. doi:10.1103/PhysRevLett.106.036102
5. Waghmare PR, Das S, Mitra SK (2013) *Soft Matter* 9:7437. doi:10.1039/C3SM50981H
6. Tuteja A, Choi W, Ma M, Mabry JM, Mazzella SA, Rutledge GC, McKinley GH, Cohen RE (2007) *Science* 318(5856):1618. doi:10.1126/science.1148326
7. Liu T, Kim CJ (2014) *Science* 346(6213):1096. doi:10.1126/science.1254787
8. Taylor M, Urquhart AJ, Zelzer M, Davies MC, Alexander MR (2007) *Langmuir* 23(13):6875. doi:10.1021/la070100j
9. Deng X, Mammen L, Butt HJ, Vollmer D (2012) *Science* 335(6064):67. doi:10.1126/science.1207115
10. Rioboo R, Marengo M, Tropea C (2002) *Exp Fluids* 33(1):112. doi:10.1007/s00348-002-0431-x
11. Vadillo D, Soucemarianadin A, Delattre C, Roux DCD (2009) *Phys Fluids* 21(122002):122002
12. Ukiwe C, Kwok DY (2005) *Langmuir* 21(2):666. doi:10.1021/la0481288
13. Pasandideh-Fard M, Qiao Y, Chandra S, Mostaghimi J (1996) *Phys Fluids* 8(3):650
14. Butt HJ, Roisman IV, Brinkmann M, Papadopoulos P, Vollmer D, Semprebon C (2014) *Current Opinion in Colloid and Interface Science* 19(4):343. doi:10.1016/j.cocis.2014.04.009
15. Weser F, Scheithauer C, Friedrich B (2015) Contact angle measurement apparatus. <https://www.google.de/patents/EP2899528A1?cl=en>. EP Patent App. EP20,140,152,563
16. Collet P, De Coninck J, Drouiche K, Dunlop F (2013) *Colloid Polym Sci* 291(2):291. doi:10.1007/s00396-012-2839-z
17. Bormashenko E (2013) *Colloid Polym Sci* 291(2):339. doi:10.1007/s00396-012-2778-8
18. Tavana H, Yang G, Yip CM, Appelhans D, Zschoche S, Grundke K, Hair ML, Neumann AW (2006) *Langmuir* 22(2):628. doi:10.1021/la051715o
19. Ashurst W, Yau C, Carraro C, Maboudian R, Dugger M (2001) *J Microelectromech Syst* 10(1):41. doi:10.1109/84.911090
20. Wang A, Tang H, Cao T, Salley SO, Ng KS (2005) *J Colloid Interface Sci* 291(2):438. doi:10.1016/j.jcis.2005.05.008
21. Bonn D, Eggers J, Indekeu J, Meunier J, Rolley E (2009) *Rev Mod Phys* 81:739. doi:10.1103/RevModPhys.81.739
22. Blake TD (2006) *J Colloid Interface Sci* 299(1):1. doi:10.1016/j.jcis.2006.03.051